Title
Fabrication of 3D high aspect ratio PDMS microfluidic networks with a hybrid stamp

Journal
Lab on a Chip, 15(8)

ISSN
1473-0197

Authors
Kung, Yu-Chun
Huang, Kuo-Wei
Fan, Yu-Jui
et al.

Publication Date
2015-04-21

DOI
10.1039/c4lc01211a

Peer reviewed

Lab on a Chip

PAPER

View Article Online
View Journal | View Issue

Cite this: *Lab Chip*, 2015, **15**, 1861

Fabrication of 3D high aspect ratio PDMS microfluidic networks with a hybrid stamp†

Yu-Chun Kung,[a] Kuo-Wei Huang,[a] Yu-Jui Fan[ab] and Pei-Yu Chiou*[a]

We report a novel methodology for fabricating large-area, multilayer, thin-film, high aspect ratio, 3D microfluidic structures with through-layer vias and open channels that can be bonded between hard substrates. It is realized by utilizing a hybrid stamp with a thin plastic sheet embedded underneath a PDMS surface. This hybrid stamp solves an important edge protrusion issue during PDMS molding while maintaining necessary stamp elasticity to ensure the removal of PDMS residues at through-layer regions. Removing edge protrusion is a significant progress toward fabricating 3D structures since high aspect ratio PDMS structures with flat interfaces can be realized to facilitate multilayer stacking and bonding to hard substrates. Our method also allows for the fabrication of 3D deformable channels, which can lead to profound applications in electrokinetics, optofluidics, inertial microfluidics, and other fields where the shape of the channel cross section plays a key role in device physics. To demonstrate, as an example, we have fabricated a microfluidic channel by sandwiching two 20 μm wide, 80 μm tall PDMS membranes between two featureless ITO glass substrates. By applying electrical bias to the two ITO substrates and pressure to deform the thin membrane sidewalls, strong electric field enhancement can be generated in the center of a channel to enable 3D sheathless dielectrophoretic focusing of biological objects including mammalian cells and bacteria at a flow speed up to 14 cm s^{-1}.

Received 14th October 2014,
Accepted 13th February 2015

DOI: 10.1039/c4lc01211a

www.rsc.org/loc

Introduction

Lab on a chip systems have attracted tremendous interest in both academic and industries in the past decade for their potential applications in personal medicine, health care, environmental monitoring, and chemical synthesis.[1] With the increasing demand of more integrated functions on a chip, advancements in manufacturing technology are critical to provide flexibility in integration of heterogeneous materials, a better interface between macro and micro components, and simple routing approaches for massively parallel fluid manipulation and control. 3D microfluidics is one of the future trends since it not only significantly increases the number of functional units that can be integrated on a chip, thus increasing the processing power and throughput, but also provides many important unique functions that are difficult to realize with conventional 2D technologies,[2–4] such as 3D sheath flows for sample focusing[5,6] and 3D tissue engineering.[7–14]

Versatile approaches have been demonstrated in the prior literature for fabricating 3D microfluidic structures. Silicon-based microfabrication allows the creation of high-resolution, high aspect ratio structures on silicon substrates, high conductivity metal electrodes for electrical sensing and actuation, and high quality semiconductor devices for IC integration. The drawbacks, however, are the high manufacturing costs and challenges to integrate with other microfluidic components. Thermal plastic hot embossing is a fast and efficient way for fabricating microfluidic structures.[15] Yet, it has residual membrane issues and cannot be used to fabricate uniform through-layer structures for interlayer communication. Photosensitive epoxy polymers such as SU-8 can be optically patterned and stacked through thermal bonding.[16–18] However, it is well known that during the spin-coating process, uneven thickness around the structures can hinder uniform bonding across a large area, which potentially leads to fluid leakage.

Multilayer soft lithography (MSL) has been widely applied for fabricating microfluidic devices in the recent decade.[19] Numerous PDMS based devices from simple monolayer PDMS channels to complex multilayer microfluidic systems with pneumatically controlled pumps and valves have been demonstrated.[20] Thousands of valves and chambers can be integrated on a chip to perform multistep biochemical analyses.[21] Most PDMS based devices, however, are not true 3D

[a] *Mechanical and Aerospace Engineering Department, University of California, Los Angeles, USA. E-mail: pychiou@seas.ucla.edu*
[b] *Institute of Applied Mechanics, National Taiwan University, Taipei, Taiwan*
† Electronic supplementary information (ESI) available: See DOI: 10.1039/c4lc01211a

devices since they do not have through-layer structures such as holes or channels for vertical fluid routing. This limitation comes from the lack of a reliable approach for fabricating through-layer structures with high resolution. Without interlayer communication structures, fluid routing, control, and sample addressing become challenges when sample size becomes large.

Several prior fabrication approaches have been demonstrated to solve the issue of fabricating interlayer communication structures, but with different degrees of success. One simple method is the use of a multilevel mold with raised post structures. By spinning a thin, uncured PDMS layer on this mold, through-layer vias can be formed at locations with these raised posts.[22] This method, although simple, does not provide large area uniformity since it is sensitive to many parameters such as via height, membrane thickness, and density of vias. To prevent the formation of residual membranes at via locations, an approach utilizing pressure gas to blow off uncured PDMS at via locations has been demonstrated as well, but there are concerns regarding the throughput and uniformity across the chip.[23]

Another approach is to utilize a soft PDMS stamp to fabricate PDMS thin films with through-layer structures and stack them layer-by-layer.[24] A soft PDMS stamp ensures the removal of the interface residues between the stamp and the mold. This approach, however, introduces an edge protrusion issue near vias due to a deformed stamp in the molding process. These nonplanar features can accumulate and limit the number of layers that can be stacked since bonding nonflat surfaces is challenging. For fine features such as narrow high-aspect-ratio structures, these protruding edges prohibit their bonding to hard substrates, and limit the structure resolution that can be fabricated. Another approach utilizing a hard glass stamp with the aid of amine surface treatment has also been demonstrated. The amine treatment can inhibit the polymerization process of a thin uncured PDMS layer adjacent to the stamp surface to remove the residual PDMS at through-layer regions.[25,26] The diffusion-based polymerization inhibition process, however, limits the structure density and resolution of layer thickness. Another approach using CO_2 laser to directly ablate through a thin PDMS film is also demonstrated. However, this approach generates rough surfaces and non-vertical sidewalls.[27]

Here, we demonstrate a hybrid stamp approach to solve the edge protrusion issue and provide a reliable method for fabricating high aspect ratio (HAR), high resolution PDMS 3D thin-film structures across a large area. HAR is defined as the ratio of structure height to width. In this approach, a PDMS stamp is embedded with a thin plastic plate underneath a chemically treated PDMS surface. This plastic plate increases the mechanical stiffness near the stamp surface to prevent severe deformation to eliminate the occurrence of protruding edges. A thin layer of elastic PDMS film on top of the plastic plate provides the required elasticity to ensure a complete removal of uncured PDMS residues at through-layer regions. Removing edge protrusion is a significant step. It permits the fabrication of high resolution, large area, high-aspect-ratio PDMS thin films with through-layer features to construct 3D microfluidic devices. Flat PDMS interfaces allow narrow HAR structures to be bonded reliably between hard substrates, on which high quality electronic, optical, and semiconductor devices are typically fabricated. This gives chip designers more flexibility in integrating heterogeneous materials, structures, devices, and systems on the same chip with more functional modules.

Fabrication of 3D microfluidic networks with a hybrid stamp

Fig. 1 shows the schematic of the process flow of fabricating 3D microfluidic structures using the hybrid stamp approach.

Step 1: fabrication of master molds

It starts from fabricating SU-8 mold masters on silicon wafers using photolithography (Fig. 1(a)). A thin SU-8 layer is coated before the thick SU-8 mold to enhance the adhesion to the bulk silicon wafer. All masters need to be surface treated with trichloro(1*H*,1*H*,2*H*,2*H*-perfluorooctyl)silane (97%, Sigma-Aldrich, USA), also called PFOCTS, to facilitate later demolding. This surface treatment was carried out in a vacuum chamber at a pressure of −30 psi for 16 hours.

Step 2: fabrication of hybrid stamps

It starts from preparing a Sylgard 184 silicone elastomer mixture (Dow Corning Corporation, Midland, USA). The ratio of base : curing agent is 10 g : 1 g. A few drops of this mixture are poured into a Petri dish. A suitable size of polystyrene plastic plate is cut and pressed against the bottom of the Petri dish under a pressure of 3 psi. A thin layer of polydimethylsiloxane (PDMS) with a thickness of roughly 30 μm is formed between the Petri dish and the plastic plate. Additional uncured PDMS is poured to fill up the Petri dish, followed by a curing step at 60 °C in an oven for 12 hours. A hybrid stamp is formed when the plastic plate together with a thin PDMS layer on its surface is peeled off from the Petri dish (Fig. 1(b)). The hybrid stamp is also surface treated with PFOCTS as in step 1 for 6 hours. To fabricate the PDMS thin film with through-layer structures, uncured PDMS is poured onto the master mold, pressed by the hybrid stamp under a pressure of 4 psi, and cured at 50 °C in an oven for an hour.

Step 3: demolding PDMS films from master mold

During the demolding process, the cured PDMS thin film has stronger adhesion to the hybrid stamp than to the master mold since more PFOCTS is coated on the master mold due to a longer treatment time (Fig. 1(c)).

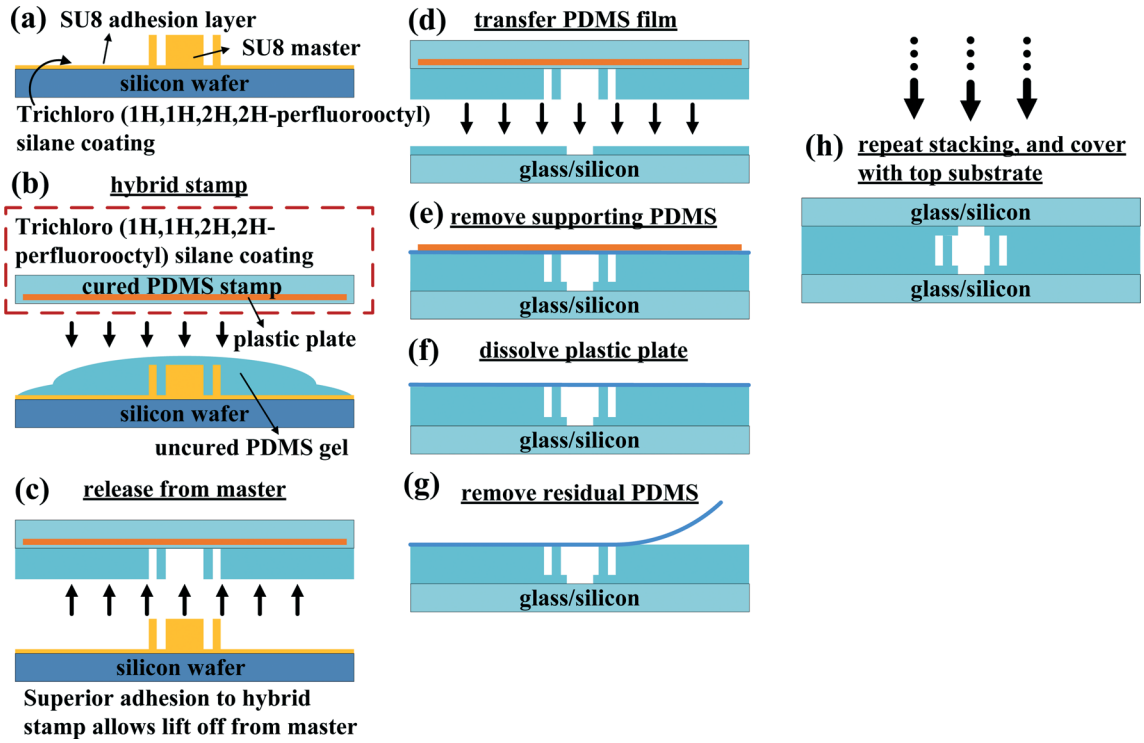

Fig. 1 Schematic of fabrication process flow using a plastic plate embedded hybrid stamp. (a) A SU8 master is treated with PFOCTS to facilitate later demolding. (b) Uncured PDMS mixture is poured on the master, and pressed against the hybrid stamp. (c) Due to less PFOCTS treatment on the hybrid stamp compared to the master, the casted PDMS film tends to adhere to the hybrid stamp and allows to be peeled off from the master. (d) The film is transferred and bonded by oxygen plasma treatment. (e) Removal of the support PDMS on the hybrid stamp. (f) Dissolving the polystyrene plastic plate in acetone. (g) Removal of the residual PDMS thin film to complete the removal of a hybrid stamp. (h) The stacking process is repeated to complete the fabrication process, which includes bonding to a hard substrate.

Step 4: transfer and stacking of PDMS thin films

Oxygen plasma treatment is performed on both the PDMS thin film on the hybrid stamp and the substrate to be bonded for two minutes. Alignment is performed under a microscope before bonding (Fig. 1(d)). The bonded set is baked in an oven at 60 °C for 2 hours.

Step 5: removing hybrid stamp

It starts from peeling off the bulk PDMS part on the plastic plate (Fig. 1(e)), followed by dissolving the polystyrene plastic plate in an acetone bath for 4 hours (Fig. 1(f)). This leaves a thin residual PDMS film on the substrate that can be easily peeled off from the device due to prior PFOCTS treatment (Fig. 1(g)) to finish the transferring and stacking process of a PDMS thin film with through-layer structures. This mechanically gentle releasing technique allows us to transfer the PDMS thin film to fragile substrates, such as a glass cover slip, over a large area.

Step 6: constructing multilayer 3D microfluidic devices

By repeating steps 1–5, multilayer 3D PDMS structures with interlayer vias and high aspect ratio structures could be constructed and bonded between two hard substrates (Fig. 1(h)).

Results and discussion

The purpose to utilize a hybrid stamp in the molding process is to remove the protruding edges of the molded PDMS structures. If the stamp is made purely of PDMS, the contact surface is relatively soft. When pressure is applied on a stamp to clear PDMS residuals at through-layer regions, the stamp at contact regions deforms. Since uncured PDMS is solidified between a deformed stamp and a mold, protruding edges are formed and transferred to the molded structures. These non-flat surfaces inhibit follow-up bonding to other structures. This problem becomes severe when small features are transferred since the protruded edges can occupy a significant area on these features. Tight contact required for good bonding between layers is not allowed. A similar deformation issue also occurs in the alternative approach of creating through-layer PDMS structures using a soft master mold and a hard stamp. In the case of a hard master mold and hard stamp combination, the uncured PDMS residuals at the through-layer regions cannot be completely removed. The novelty of the plastic embedded hybrid stamp is to provide a stiff stamp to prevent deformation, while keeping a required elasticity at the contact interface to ensure a complete removal of uncured PDMS at through-layer regions. The plastic plate has a Young's modulus of E = 3.2 GPa, much larger than the PDMS Young's modulus (E = 0.6 MPa).

Fig. 2(a, b) and (c, d) show the degree of edge deformation of PDMS structures molded by a standard PDMS stamp and a hybrid stamp, respectively. In Fig. 2(d), an open microfluidic channel with HAR (5 : 1) PDMS walls is demonstrated. Fig. 3 shows a multilayer PDMS structure with pneumatically driven microvalves sandwiched between two hard, transparent, and electrically conductive ITO glass substrates. In addition, a 30 μm thick PDMS membrane with a high-density

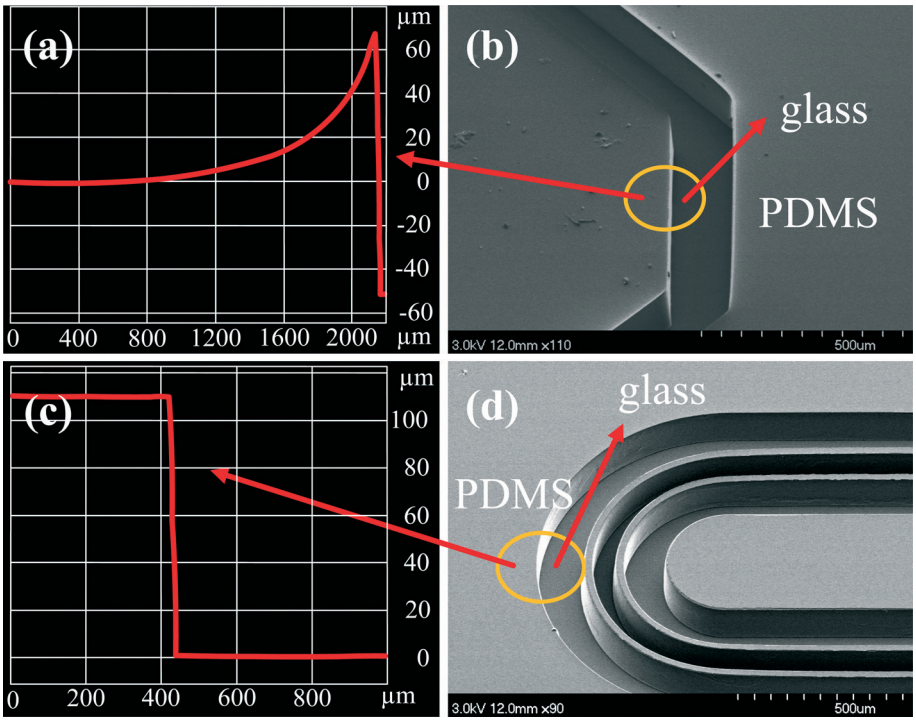

Fig. 2 (a, b) Edge protrusion issue near open structures of a PDMS thin film fabricated with a standard elastic PDMS stamp. This issue can be eliminated by using a plastic sheet embedded hybrid stamp in the molding process as shown in (c, d). Without the embedded plastic sheet, the contact surface is soft and results in protrusion edges around the channel. With the hybrid stamp, the contact surface is much more rigid to prevent the edge protrusion, and retains its ability to handle freestanding HAR sidewall structure.

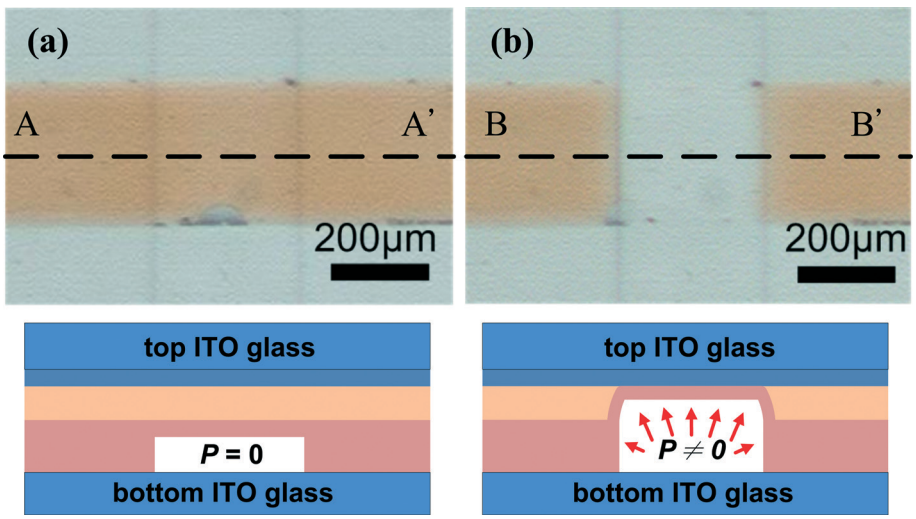

Fig. 3 Two layers of thin film PDMS structure with integrated pneumatic microvalve are bonded and sandwiched between two ITO coated glass substrates. (a) The top layer with fluidic channels is filled with dye liquid. The bottom layer is filled with uncolored DI water. The pneumatic pressure applied to the bottom channel is $P = 0$, which causes no valve membrane deformation. The subset shows the cross-sectional view along the AA′ line. (b) When a sufficient pneumatic pressure P is applied to the bottom channel, the valve membrane deforms and fully closes the top channel. The subset shows the cross-sectional view along the BB′ line.

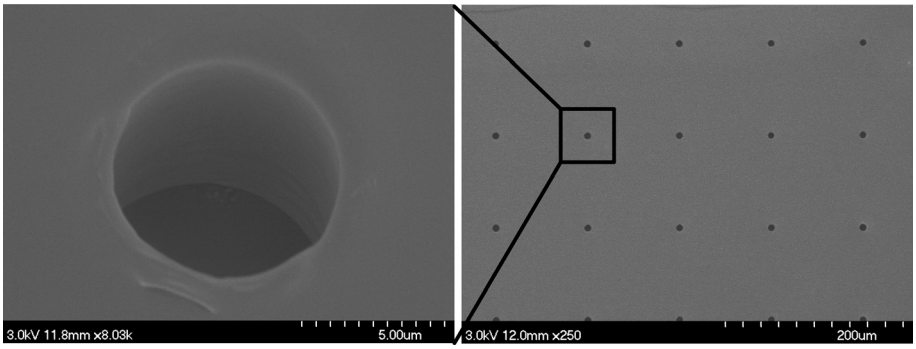

Fig. 4 SEM images of a 30 μm thick PDMS membrane with an array of 6 μm wide through-layer holes.

array of HAR through-layer vias that are 6 μm in diameter has also been successfully fabricated, as shown in Fig. 4. The pitch between vias is 100 μm. Table S1 in the ESI† summarizes recent representative reports on fabrication of 3D microfluidic structures. Parameters including lateral resolution, layer thickness resolution, hard substrate bonding ability, interlayer deformable structure, vias, and HAR value are provided for comparison with the current work. The resolution and HAR value of our current approach is limited by the resolution of photolithography for making the master mold. To create a HAR structure with a lateral resolution of 6 μm, the maximum thickness we can achieve is 30 μm due to the optical diffraction limit when patterning a thick photoresist.

High aspect ratio deformable membranes for 3D dielectrophoresis focusing

In addition to providing three-dimensional fluid routing, the ability to fabricate vertical, thin, HAR PDMS membranes and bond them to hard substrates allows the fabrication of deformable channels. This unique advantage promises novel functional devices not possible before, especially in fields such as electrokinetics, optofluidics, and inertial microfluidics, in which the channel cross section profile plays a critical role in underlying device physics. For example, particle focusing equilibrium locations can change in a high-speed inertial flow when the channel deforms; and a curved and deformed channel can work as a tunable lens for light focusing and collection in optofluidics.

Here, we demonstrate a novel electrokinetic device that can achieve tunable 3D cell focusing in the center of a channel without sheath flows. Fig. 5(a, b) show the schematic of such a device fabricated using the hybrid stamp approach. A single layer PDMS thin film with high aspect ratio (HAR = 4) walls is bonded between two featureless ITO glass substrates. Fig. 5(c) shows the picture of a completed microfluidic device. By applying pressure to the two side channels, the middle channels can be deformed as shown in Fig. 5(b). Application of an electrical bias to the two featureless ITO electrodes causes electric field streamlines to be focused in the middle neck of the deformed channel, creating a highly non-uniform electric field distribution with the maximum field enhancement occurring in the center (Fig. 5(d)).

Fig. 6(a) and (b) show the microscope images of a channel with vertical sidewalls 80 μm high and 20 μm thick before and after a pressure of 60 psi is applied to the side channels. Video S1 in the ESI† shows the tunable channel deformation when different pneumatic pressure values were applied to the side channel. An alternating current (a.c.) signal is applied to the top and bottom ITO electrodes to provide the electric field required for cell focusing using dielectrophoresis.

Dielectrophoresis (DEP) is a phenomenon in which a particle in a non-uniform electric field can experience an electrostatic force moving the particle towards stronger electric field regions if the particle is more polarizable than the medium, called positive DEP. A particle moves to weaker electric field regions if the particle is less polarizable than the medium, called negative DEP.[28–33] To migrate a particle in an electric field using dielectrophoresis, there must be an electric field gradient. In a uniform electric field region, although particles are polarized, no net DEP forces can be induced for moving.

Fig. 6(c) and (d) compare the simulated electric field distribution in a channel without and with deformation, respectively. Since the sidewalls can be continuously deformed to eventually contact each other and seal the gap, this device allows the tuning of electric field strength in the middle of the channel by controlling the applied pressure in the side channels. The narrower the neck, the larger the electric field enhancement is generated in the neck. This allows the creation of strong electric field gradients for focusing small objects such as bacteria. Cells or particles experiencing positive DEP forces in the channel are attracted to the center of the channel, providing a continuous 3D sheathless cell focusing function for potential applications in microfluidic flow cytometers and cell sorters.

The performance of 3D DEP focusing on this deformable channel is tested using two types of cells, GFP-HeLa with a diameter of 15 μm and GFP-*E. coli* with rod shape of 2 μm long and 700 nm diameter. Before pumping the sample into the device, GFP-HeLa cells were suspended in an isotonic buffer consisting of 8.5% sucrose and 0.3% dextrose and with a conductivity of 10 mS m^{-1}. GFP-*E. coli* was suspended in a buffer solution of 10% sucrose in 20 mM HEPES and

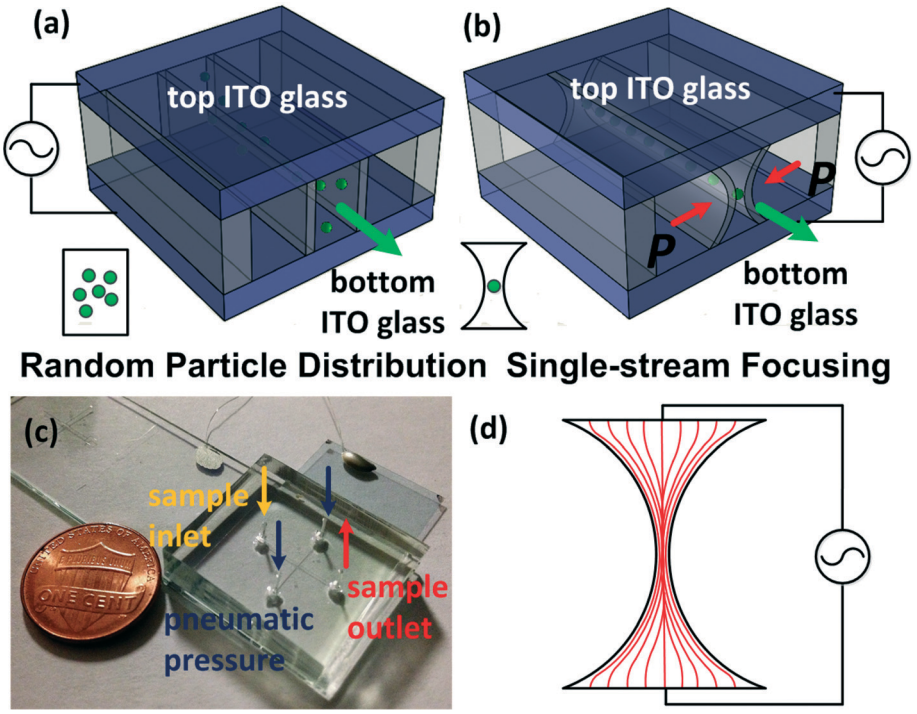

Fig. 5 Schematic of a tunable 3D DEP focusing device. (a) An open PDMS microchannel with thin, high-aspect-ratio sidewalls is sandwiched between two conductive indium tin oxide (ITO) coated glass substrates. An a.c. signal is applied between the top and bottom substrate. (b) When the channel sidewalls are pressurized, the channel deforms to form a narrow neck in the middle and focus the electric field lines. Positive DEP responding particles would migrate to the center of the channel where the maximum electric field occurs. (c) Photograph of a fabricated device. (d) A schematic showing crowding electric field streamlines in the neck of a deformed channel.

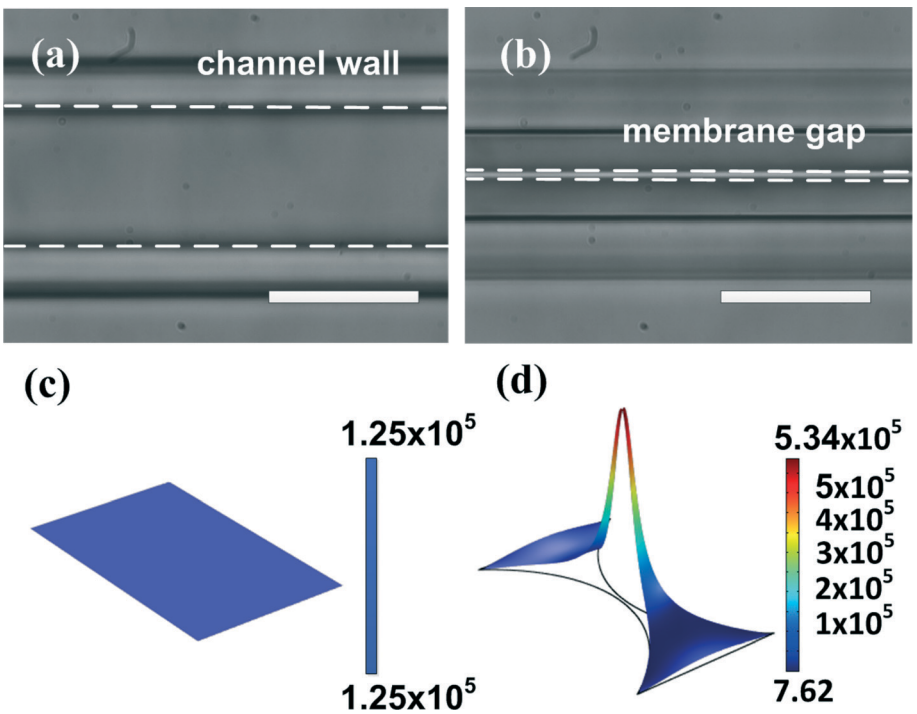

Fig. 6 (a) Microscopy images of a deformable microchannel with dimensions 50 μm in width, 80 μm in height, and a sidewall thickness of 20 μm. (b) The channel sidewalls are under a pressure of 60 psi. (c) Electric field distribution in a microchannel without deformation under an ac bias of 10 V peak-to-peak at a frequency of 5 MHz. (d) When the channel is deformed to form a neck that is only 0.5 μm wide, strong field enhancement is generated in the middle of this channel. Scale bar: 50 μm.

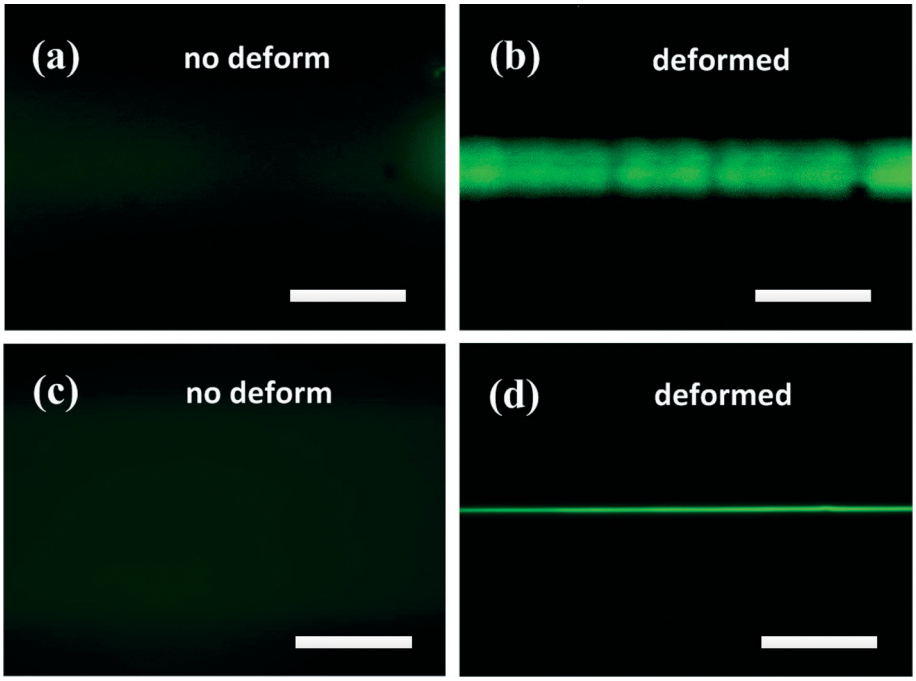

Fig. 7 The focused fluorescence traces of biological objects. All samples are suspended in media with conductivities ranging from 10 mS m^{-1} to 30 mS m^{-1}. An a.c. signal of 56.6 V peak-to-peak with frequencies varying from 300 kHz to 5 MHz is applied. (a, b) Comparison of the fluorescence traces of GFP-HeLa (spherical shape, 15 μm in diameter) in a channel without and with sidewall deformation (35 psi) at an average flow speed of 17 cm s^{-1}. The channel neck in (b) is 16 μm; (c, d) comparison of the traces of GFP-*E. coli* (rod-shaped, 2 μm long and 700 nm wide) in a channel without and with sidewall deformation (60 psi) at an average flow speed of 14 cm s^{-1}. The channel neck in (d) is 3 μm. Scale bar: 25 μm.

with a conductivity of 30 mS m^{-1}. The sample was injected continuously into the microchannel by a syringe pump (KD Scientific, 780100). A function generator (Agilent, 33220A) and power amplifier (ENI, Model 2100L) were used to provide the a.c. voltage source. The DEP response of the cells was monitored under an inverted fluorescence microscope (Carl Zeiss, Axio Observer.A1), and recorded by a CCD camera (Carl Zeiss, AxioCam MRm). For the HeLa-GFP focusing, the side channels were pressurized at 35 psi to create a 16 μm wide gap, roughly the size of HeLa cells. When an a.c. signal (300 kHz, 56.6 V peak-to-peak) was applied, GFP-HeLa cells were focused to the center of the channel (Fig. 7(b)), and remained focused in downstream even at regions without deformed channels due to the laminar flow nature in microfluidics. To focus *E. coli*, the sidewalls of the channel are further deformed to a smaller gap of only 3 μm to create a stronger electric field strength and gradient for focusing these smaller objects. Under the application of an a.c. signal (5 MHz, 56.6 V peak-to-peak), when there is no sidewall deformation, GFP-*E. coli* was randomly distributed across the channel (Fig. 7(c)). When side channels were pressurized at 60 psi to create a 3 μm gap, positive DEP force focused GFP-*E. coli* to the center of the channel to form a single-stream fluorescence trace as shown in Fig. 7(d) and video S2 in the ESI.†

Conclusion

This paper demonstrates a new fabrication approach capable of manufacturing multilayer, 3D, HAR, open PDMS based microfluidic structures that can be bonded between hard substrates. This approach utilizes a hybrid stamp that consists of a plastic plate embedded right underneath a thin PDMS film to provide the required hardness for preventing severe stamp deformation during molding processes. A thin layer of PDMS film on the plastic plate provides local elasticity to ensure a complete removal of uncured residual PDMS in the through-layer regions. HAR PDMS structures fabricated by this method do not have protruding edges and offer flat interfaces for multilayer stacking and bonding to hard substrates. Using this unique fabrication capability, we demonstrate deformable channels formed by sandwiching thin, vertical, HAR PDMS channel walls between two ITO substrates. These thin channel sidewalls can be continuously deformed under pressure to change the cross section of a channel, a feature that may find many applications in fields such as optofluidics, inertial microfluidics, and electrokinetics that have channel profile sensitive physical phenomena. To demonstrate, we utilized this deformable channel structure to achieve single stream, 3D, sheathless focusing of mammalian cells and small bacteria.

Acknowledgements

This work is supported by NSF DBI 1256178, NSF ECCS1232279, and Cal. Cap. LLC through an industry research agreement.

References

1 L. Y. Yeo, *et al.*, Microfluidic Devices for Bioapplications, *Small*, 2011, **7**(1), 12–48.
2 J. Shi, S. Yazdi, S.-C. Steven Lin, X. Ding, I.-K. Chiang, K. Sharp and T. J. Huang, Three-dimensional continuous particle focusing in a microfluidic channel via standing surface acoustic waves (SSAW), *Lab Chip*, 2011, **11**, 2319–2324.
3 J. Shi, X. Mao, D. Ahmed, A. Colletti and T. J. Huang, Focusing microparticles in a microfluidic channel with standing surface acoustic waves (SSAW), *Lab Chip*, 2008, **8**, 221–223.
4 Y. Chen, A. A. Nawaz, Y. Zhao, P.-H. Huang, J. P. McCoy, S. J. Levine, L. Wang and T. J. Huang, Standing surface acoustic wave (SSAW)-based microfluidic cytometer, *Lab Chip*, 2014, **14**, 916–923.
5 Y. Chen, *et al.*, 3D pulsed laser-triggered high-speed microfluidic fluorescence-activated cell sorter, *Analyst*, 2013, **138**, 7308–7315.
6 Y. J. Fan, *et al.*, Three dimensional microfluidics with embedded microball lenses for parallel and high throughput multicolor fluorescence detection, *Biomicrofluidics*, 2013, **7**(4), 044121.
7 D. Huh, *et al.*, Reconstituting Organ-Level Lung Functions on a Chip, *Science*, 2010, **328**(5986), 1662–1668.
8 Y.-H. Jang, *et al.*, An integrated microfluidic device for two-dimensional combinatorial dilution, *Lab Chip*, 2011, **11**(19), 3277–3286.
9 J. Kim, *et al.*, A programmable microfluidic cell array for combinatorial drug screening, *Lab Chip*, 2012, **12**(10), 1813–1822.
10 M. C. Liu, D. Ho and Y.-C. Tai, Monolithic fabrication of three-dimensional microfluidic networks for constructing cell culture array with an integrated combinatorial mixer, *Sens. Actuators, B*, 2008, **129**(2), 826–833.
11 M. C. Liu and Y.-C. Tai, A 3-D microfluidic combinatorial cell array, *Biomed. Microdevices*, 2011, **13**(1), 191–201.
12 E. Ostuni, *et al.*, Patterning Mammalian Cells Using Elastomeric Membranes, *Langmuir*, 2000, **16**(20), 7811–7819.
13 Y. Wang, *et al.*, Capture and 3D culture of colonic crypts and colonoids in a microarray platform, *Lab Chip*, 2013, **13**(23), 4625–4634.
14 C. W. Gregory, *et al.*, High yield fabrication of multilayer polydimethylsiloxane devices with freestanding micropillar arrays, *Biomicrofluidics*, 2013, **7**(5), 0565503.
15 D. Brassard, *et al.*, 3D thermoplastic elastomer microfluidic devices for biological probe immobilization, *Lab Chip*, 2011, **11**(23), 4099–4107.
16 M. Agirregabiria, *et al.*, Fabrication of SU-8 multilayer microstructures based on successive CMOS compatible adhesive bonding and releasing steps, *Lab Chip*, 2005, **5**, 545–552.
17 J. N. Patel, *et al.*, SU-8- and PDMS-based hybrid fabrication technology for combination of permanently bonded flexible and rigid features on a single device, *J. Micromech. Microeng.*, 2013, **23**(6), 065029.
18 J. N. Patel, *et al.*, PDMS as a sacrificial substrate for SU-8-based biomedical and microfluidic applications, *J. Micromech. Microeng.*, 2008, **18**, 095028.
19 M. A. Unger, *et al.*, Monolithic Microfabricated Valves and Pumps by Multilayer Soft Lithography, *Science*, 2000, **288**(5463), 113–116.
20 J. W. Hong and S. R. Quake, Integrated nanoliter systems, *Nat. Biotechnol.*, 2003, **21**, 1179–1183.
21 T. Thorsen, S. J. Maerkl and S. R. Quake, Microfluidic Large-Scale Integration, *Science*, 2002, **298**(5593), 580–584.
22 E. P. Kartalov, *et al.*, Microfluidic vias enable nested bioarrays and autoregulatory devices in Newtonian fluids, *Proc. Natl. Acad. Sci. U. S. A.*, 2006, **103**(33), 12280–12284.
23 J. H. Kang, E. Um and J.-K. Park, Fabrication of a poly(dimethylsiloxane) membrane with well-defined through-holes for three-dimensional microfluidic networks, *J. Micromech. Microeng.*, 2009, **19**, 045027.
24 M. Zhang, *et al.*, A simple method for fabricating multi-layer PDMS structures for 3D microfluidic chips, *Lab Chip*, 2010, **10**(9), 1199–1203.
25 C. F. Carlborg, *et al.*, A High-Yield Process for 3-D Large-Scale Integrated Microfluidic Networks in PDMS, *J. Microelectromech. Syst.*, 2010, **19**(5), 1050–1057.
26 J. M. Karlsson, *et al.*, Fabrication and transfer of fragile 3D PDMS microstructures, *J. Micromech. Microeng.*, 2012, **22**(8), 085009.
27 M. Li, *et al.*, A simple and cost-effective method for fabrication of integrated electronic-microfluidic devices using a laser-patterned PDMS layer, *Microfluid. Nanofluid.*, 2012, **12**(5), 751–760.
28 K. Khoshmanesh, *et al.*, Dielectrophoretic Platforms for Bio-microfluidic Systems, *Biosens. Bioelectron.*, 2011, **26**(5), 1800–1814.
29 R. Pethig, Review Article—Dielectrophoresis: Status of the theory, technology, and applications, *Biomicrofluidics*, 2010, **4**(2), 022811.
30 I. Barbulovic-Nad, *et al.*, DC-dielectrophoretic separation of microparticles using an oil droplet obstacle, *Lab Chip*, 2006, **6**(2), 274–279.
31 E. B. Cummings and A. K. Singh, Dielectrophoresis in Microchips Containing Arrays of Insulating Posts: Theoretical and Experimental Results, *Anal. Chem.*, 2003, **75**(18), 4724–4731.
32 K. H. Kang, *et al.*, Continuous separation of microparticles by size with Direct current-dielectrophoresis, *Electrophoresis*, 2006, **27**(3), 694–702.
33 A. Salmanzadeh, *et al.*, Isolation of prostate tumor initiating cells (TICs) through their dielectrophoretic signature, *Lab Chip*, 2011, **12**(1), 182–189.